FEBS Letters 581 (2007) 4298–4302

Structural element responsible for the Fe(III)–phytosiderophore specific transport by HvYS1 transporter in barley

Emiko Harada, Kenji Sugase, Kosuke Namba[1], Takashi Iwashita, Yoshiko Murata*

Suntory Institute for Bioorganic Research, 1-1-1 Wakayamadai, Shimamoto-cho, Mishima-gun, Osaka 618-8503, Japan

Received 4 July 2007; revised 3 August 2007; accepted 3 August 2007

Available online 13 August 2007

Edited by Richard Cogdell

Abstract ***Hordeum vulgare*** **L. yellow stripe 1 (HvYS1) is a selective transporter for Fe(III)–phytosiderophores, involved in primary iron acquisition from soils in barley roots. In contrast, *Zea mays* yellow stripe 1 (ZmYS1) in maize possesses broad substrate specificity, despite a high homology with HvYS1. Here we revealed, by assessing the transport activity of a series of HvYS1–ZmYS1 chimeras, that the outer membrane loop between the sixth and seventh transmembrane regions is essential for substrate specificity. Circular dichroism spectra indicated that a synthetic peptide corresponding to the loop of HvYS1 forms an α-helix in solution, whereas that of ZmYS1 is flexible. We propose that the structural difference at this particular loop determines the substrate specificity of the HvYS1 transporter.**

Keywords: Chimera; α-helix; Iron acquisition; Iron–phytosiderophore; Substrate specificity; Transporter

1. Introduction

Iron (Fe) is an essential element for all living organisms, with most creatures in the animal kingdom dependent on plants as their dietary sources of Fe [1–3]. Availability of Fe often limits plant growth, particularly in alkaline soils, because iron forms insoluble $Fe(OH)_3$ at high pH, resulting in very low solubility.

Under Fe-deficiency conditions, the roots of graminaceous plants secrete phytosiderophores which are hexadentate metal chelators for Fe(III) with high affinity [4,5]. The resulting Fe(III)–phytosiderophore complexes are then absorbed into the roots through specific transporter proteins. Since mugineic acid (MA) was identified in barley [6] as the first phytosiderophore, nine analogs including deoxymugineic acid (DMA) have been isolated from various graminaceous species and cultivars [7]. In plant tissues, nicotianamine (NA), a biosynthetic precursor of DMA and MA, chelates Fe(II) and other divalent metals. The Fe(II)–NA complex plays a major role in the intracellular and intercellular transport of Fe(II) ions in plant [8–10].

Membrane trafficking of metal-chelator complexes is mediated by YS1 (yellow stripe 1)/YSL (yellow stripe 1-like) transporter family. In spite of the high homology among the YS1/YSL family proteins, many of their members possess different substrate specificities. Maize (*Zea mays*) yellow stripe 1 (ZmYS1), which is the first identified transporter [11], transports various ions including Fe(III), Fe(II), Ni(II), Zn(II), Cu(II), Mn(II), and Cd(II) as their phytosiderophore complexes. In addition, ZmYS1 also transports Fe(II)–NA and Ni(II)–NA complexes [9,12]. Interestingly, HvYS1 in barley (*Hordeum vulgare* L.), which is the closest homolog of ZmYS1 with 72.7% amino acid sequence identity and 95.0% similarity, specifically transports Fe(III)–phytosiderophore complexes [12]. HvYS1 conveys neither Fe(II)–NA nor phytosiderophores in complex with any divalent metals.

The distinct difference in the substrate specificities between ZmYS1 and HvYS1 motivated us to investigate the mechanism by which these transporters distinguish between substrates. The aim of the present study is to identify the region essential for Fe(III)–phytosiderophore specificity of HvYS1 using HvYS1–ZmYS1 chimeric proteins, which were constructed by exchanging low-homology regions; an N-terminal fragment and outer membrane loop connecting the sixth and seventh transmembrane regions. Our experiments showed that one of the outer membrane loops is essential and sufficient for substrate specificity of HvYS1, while the N-terminal region of the protein has no definite influence on its substrate specificity. A synthetic peptide corresponding to the outer membrane loop in HvYS1 forms an α-helix, but that of the corresponding region in ZmYS1 has no structure in solution.

2. Materials and methods

2.1. *Electrophysiological studies in* Xenopus laevis *oocytes*

HvYS1–ZmYS1 chimeric transporters were constructed by the exchange of N-terminal regions (residues 1–313 for HvYS1 and 1–316 for ZmYS1), C-terminal regions (residues 386–678 for HvYS1 and 390–682 for ZmYS1) or middle regions (residues 314–385 for HvYS1 and 317–389 for ZmYS1) between *HvYS1* and *ZmYS1* since *Kpn*I and *Bgl*II cloning sites are conserved (Fig. 2A). The cDNA fragments were inserted into the *Xenopus* oocyte expression vector pSP64 poly A (Promega, USA) using the *Xba*I and *Bam*HI sites. The plasmids were linearized by *Bam*HI, and cRNA were transcribed *in vivo* with SP6 poly A (mMESSAGE mMACHINE kit, Ambion, USA). The cRNA solutions (50 nl, 0.1 μg μl^{-1}) were injected into the oocytes and then incubated for 2–4 days at 16 °C in ND96 buffer (pH 7.6). The electrophysiological studies in the oocytes were carried out as previously

*Corresponding author. Fax: +81 75 962 2115.
E-mail address: murata@sunbor.or.jp (Y. Murata).

[1]Present address: Faculty of Pharmaceutical Sciences, Tokushima Bunri University, Nishihama, Yamashiro-cho, Tokushima 770-8514, Japan.

Abbreviations: HvYS1, *Hordeum vulgare* L. yellow stripe 1; ZmYS1, *Zea mays* yellow stripe 1; YSL, yellow stripe 1-like; MA, mugineic acid; DMA, 2′-deoxymugineic acid; NA, nicotianamine; CD, circular dichroism

0014-5793/$32.00
doi:10.1016/j.febslet.2007.08.011

described [12]. DMA was chemically synthesized as described by Namba et al. [13] and NA was purchased from T. Hasegawa Co., Ltd. (Japan). The Fe(III)–DMA and Fe(II)–NA complexes were prepared as described in [9,12].

2.2. Peptide synthesis

The peptides DDTVSLEELHRQEIFKRGHI-NH_2 (HvYS1pep; residues 373–392 of HvYS1) and DEMAALDDLQRDEIFSDGSF-NH_2 (ZmYS1pep; residues 377–396 of ZmYS1) were prepared by solid phase synthesis using a peptide synthesizer 433A (Applied Biosystems, USA). The products were deprotected and purified by reversed phase HPLC on CAPCELL PAK C18 column (Shiseido, Japan) with an 18–42% acetonitrile gradient containing 0.1% trifluoroacetic acid. The identity and integrity of the synthetic peptides were confirmed by a Voyager matrix assisted laser desorption/ionization-time of flight-mass spectrometry (MALDI-TOF-MS, Applied Biosystems). The samples were dialyzed against 500 mL buffer containing 20 mM Tris–HCl (pH 7.0), 50 mM NaCl, and 2 mM NaN_3.

2.3. α-Helix prediction and the measurement of circular dichroism spectra

The AGADIR program (http://www.embl-heidelberg.de/Services/serrano/agadir/agadir-start.html) [14] was employed to predict the helical propensities of the peptides. The predictions were run at pH 7.0, with an ionic strength of 0.1 M at a temperature of 298 K.

The concentrations of both peptides were adjusted to 15 μM and circular dichroism (CD) spectra were recorded on a JASCO J-715 spectropolarimeter (JASCO, Japan) at 25 °C under N_2 atmosphere in a 0.5 cm-

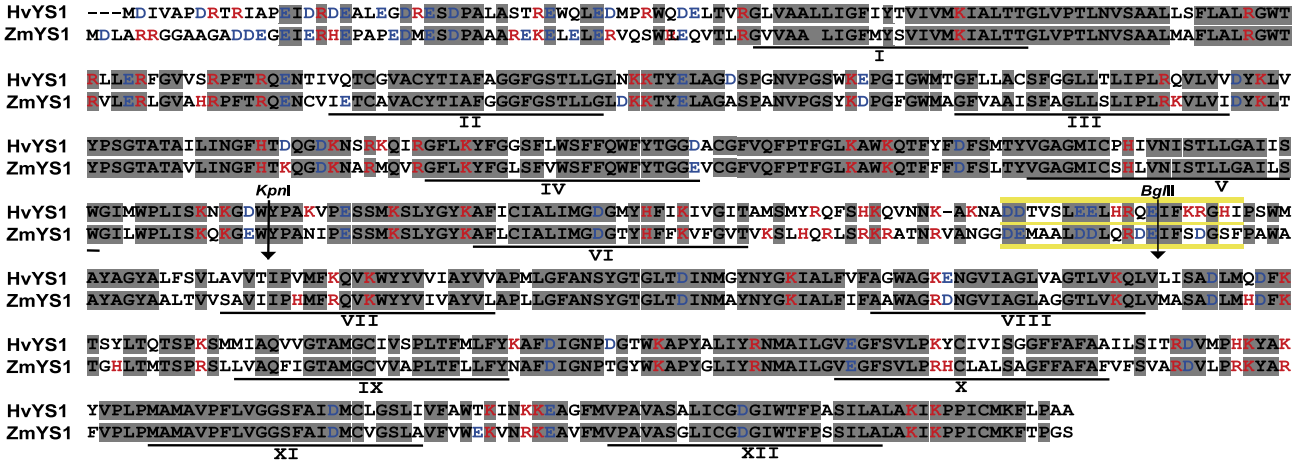

Fig. 1. Comparison of amino acid sequences of HvYS1 and ZmYS1. Accession numbers of the protein sequences deposited in the Genbank database are AB214183 (HvYS1) and AF186234 (ZmYS1). Twelve transmembrane regions of ZmYS1, predicted by the SOSUI program [16], are underlined. Acidic amino acid residues (aspartic acid, D; glutamic acid, E) are represented in blue and basic amino acids residues (histidine, H; lysine, K; arginine, R) in red. The consensus sequences are indicated by gray boxes, and amino acid residues corresponding to the synthetic peptides, HvYS1pep and ZmYS1pep, are highlighted in yellow.

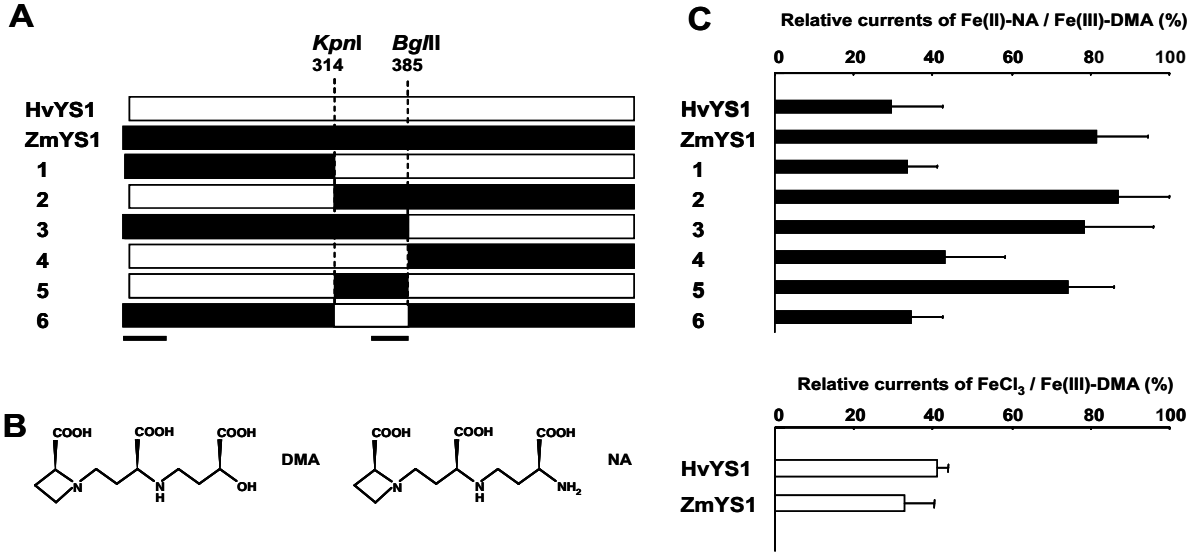

Fig. 2. HvYS1–ZmYS1 chimeras and their transport activities. (A) Schematic representation of the wild-type HvYS1 and ZmYS1 and 6 chimeric proteins. Residues 317–389 of ZmYS1 are aligned with residues 314–385 of HvYS1. Low-homology regions are underlined. (B) Structures of DMA and NA used as Fe chelators. (C) Transport activity of the wild-type HvYS1 and ZmYS1, and chimeric proteins **1**–**6** by two-electrode voltage clamp analysis in *Xenopus* oocytes. Currents induced by 50 μM Fe(III)–DMA, Fe(II)–NA or $FeCl_3$ in oocytes. Relative currents to Fe(III)–DMA are shown. Error bars show S.D. The experiment repeated 4–14 times.

cylindrical cuvette with 2 mL sample volume. Forty scans were collected for each spectrum from 300 to 190 nm. The CD spectra were analyzed by the SELCON3 algorism in the CDPro software package [15].

3. Results

The sequence homology of HvYS1 and ZmYS1 in the N-terminal outer membrane regions and the loops between the sixth and seventh transmembrane helices are significantly lower than the other regions (Fig. 1). To identify the critical regions for the substrate selectivity, we created a series of HvYS1–ZmYS1 chimeric proteins (Fig. 2A). The chimeras were expressed heterologously in *Xenopus laevis* oocytes. The oocytes were voltage-clamped and then superfused with buffer containing 50 μM Fe(III)–DMA or Fe(II)–NA (Fig. 2B and C). All chimeric constructs as well as the wild-type HvYS1 and ZmYS1 showed similar Fe(III)–DMA transport activities (Supplementary Fig. S1). The results show that all constructs function properly and the Fe(III)–DMA transport activity is not affected by the interchange, either in the variable N-terminal region or in the particular outer membrane loop. The relative currents of Fe(II)–NA/Fe(III)–DMA are shown in Fig. 2C since variation in transporter expression hampered the quantitative analysis of the response of each oocyte to Fe(II)–NA. Chimeras **2**, **3** and **5**, harboring the ZmYS1 outer membrane loop, transported Fe(II)–NA as much as Fe(III)–DMA, whereas chimeras **1**, **4** and **6** that contain the HvYS1 loop show low activities in Fe(II)–NA transport comparable with those in $FeCl_3$ for wild-type HvYS1 and ZmYS1 (Fig. 2C). The results indicate that residues 314–385 in HvYS1 are responsible for the higher selectivity of Fe(III)-DMA over Fe(II)–NA. On the other hand, the replacement of the only N-terminal region of HvYS1 with that of ZmYS1 (chimeras **1** and **2**) did not alter the selectivity of the original protein. We concluded that the variable regions in the middle outer membrane loops are essential and sufficient to define the transport specificity, whereas the N-terminal regions have no influence on the substrate specificity.

In order to examine the structural differences in the outer membrane loops between these two proteins, we calculated their helical propensities by AGADIR. Higher helical propensity was estimated for the HvYS1 segment than for the ZmYS1 segment (Fig. 3A). Extensive AGADIR predictions suggested that twenty amino acids of HvYS1 (residues 373–392) were the minimal length to maintain the high helical propensity (data not shown). Based on these results, we synthesized the peptides, HvYS1pep (residues 373–392) and ZmYS1pep (residues 377–396) (Fig. 3A), and measured their CD spectra (Fig. 3B). The helical contents were estimated to be 40% for HvYS1pep and 0% for ZmYS1pep by the SELCON3 algorithm [15].

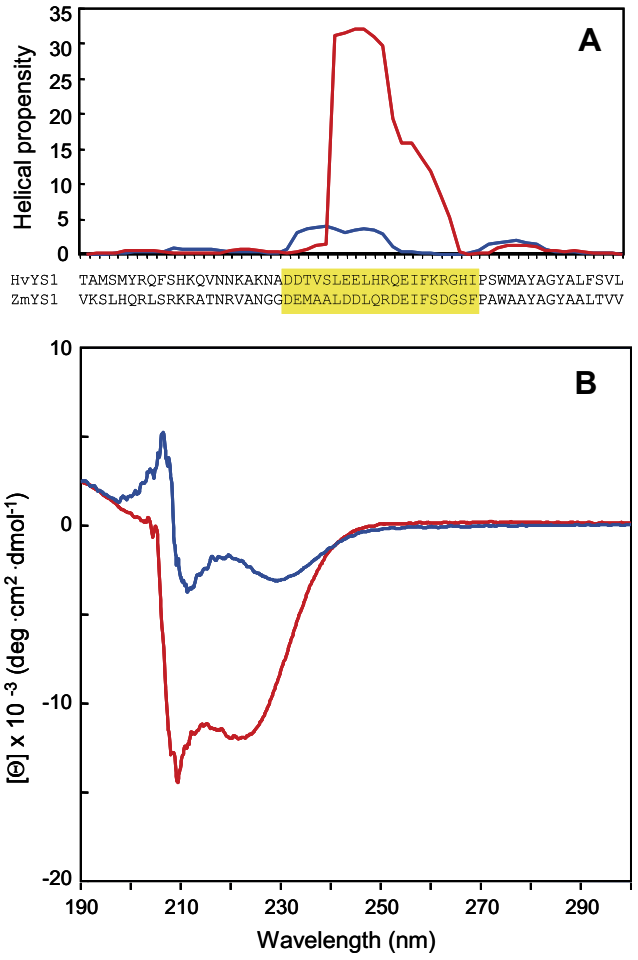

Fig. 3. Helical propensities of the outer membrane regions in HvYS1 (red) and ZmYS1 (blue). Amino acid sequences of HvYS1pep and ZmYS1pep are highlighted in yellow (A). CD spectra of HvYS1pep (red) and ZmYS1pep (blue). The buffer spectrum has been subtracted from both sample spectra (B).

4. Discussion

Phytosiderophores such as DMA are secreted from the roots of graminaceous plants to solubilize and absorb Fe(III) in soils as their complexes. On the other hand, NA is not secreted and is thought to play a role in the internal transport of Fe and other metals. Proteins of the YS1/YSL family are implicated in transports of these metal-chelator complexes. The genes of this family were cloned and characterized in several plants, including rice (*Oryza sativa*) [17], barley (*H. vulgare*) [12], Arabidopsis [18–21], tobacco (*Nicotiana tabacum*) [22], and *Thlaspi caerulescens* [23] (Supplementary Fig. S2). These transporters possess specific localizations and functions for Fe acquisition (Supplementary Table S1). For instance, OsYSL2 of rice is strongly expressed in the phloem and regulates Fe-nutrient. Electrophysiological measurements using *Xenopus* oocytes showed that OsYSL2 transports Fe(II)- and Mn(II)-NA, but not Fe(III)-chelators [17]. The YS1/YSL family proteins including HvYS1 and ZmYS1 have the most variable regions in the loops we have focused on (Supplementary Fig. S2). We predicted the α-helix percentages of the putative transmembrane loops of YS1/YSL proteins listed in Table S1 by AGADIR. Interestingly, HvYS1 has a much higher α-helix percentage (32.1) than others (1.9–5.1). Further structural studies will elucidate the correlation between the helicity of the loop and the substrate specificity of YS1/YSL family. Furthermore, the loops contain a large number of charged residues compared to other regions. Since trivalent metal–phytosiderophore complexes have different net charges from divalent metal ones [24], the charged residues in the variable outer membrane loops would be expected to participate in substrate recognition.

Our present results provide new insights into the mechanism by which Fe(III)–phytosiderophore and Fe(II)–NA are specifically recognized by the YS1/YSL family proteins. The outer membrane loop of HvYS1 is responsible for the distinct specificity for Fe(III)–phytosiderophore, but the N-terminal region does not contribute to the specificity. The CD spectra indicated that HvYS1pep forms an α-helix structure, which is expected to be operative in substrate recognition. It is noteworthy that the barley roots in which HvYS1 is strongly expressed uptake Fe(III)–MA 60 times more efficiently than Co(III)–MA [25], although the structural difference between Fe(III)–MA and Co(III)–MA is considered to be small. Therefore, in addition to the composition of the charged residues, the α-helix structure in the outer membrane loop of HvYS1 would be important for facilitating selective transportation of the Fe(III)–phytosiderophore. The membrane dynamics for metal–phytosiderophore influx/efflux systems needs further clarification with structural biological studies. This work provides us with an additional piece of the puzzle, and NMR-based studies are currently underway in our laboratory.

The World Health Organization (WHO) estimates that two billion people have Fe-deficiency anemia [2]. The increase in plant Fe content improves nutrient value. Alternatively, plants often suffer from Fe deficiency, especially when grown in calcareous soils [26]. Takahashi et al. [27] first reported that the transgenic rice produced by the heterologus expression of barley NA aminotransferase, which is an enzyme involved in the biosynthesis of DMA, becomes tolerant to low iron availability. Ferric chelate reductase also conferred both Fe-deficiency tolerance to rice and soybean and enhanced their Fe-accumulations [28,29]. Our study may shed light on solving the Fe-deficiency problems in both human and plants.

Acknowledgements: The authors thank Drs. Elsbeth L. Walker for providing the *ZmYS1* cDNA, Miki Hisada for measuring MALDI-TOF-MS, Tsuyoshi Kawada, Toshio Takahashi, and Nahoko Yamaji for their invaluable technical advice, and Dr. Honoo Satake and Prof. Shoichi Kusumoto for their fruitful discussions. This work was supported by Grants-in-Aid for Scientific Research (Grant Nos. 18710191 and 18510200). We also acknowledge the financial support of Suntory Co., Inc.

Appendix A. Supplementary data

Supplementary data associated with this article can be found, in the online version, at doi:10.1016/j.febslet.2007.08.011.

References

[1] Colangelo, E.P. and Guerinot, M.L. (2006) Put the metal to the petal: metal uptake and transport throughout plants. Curr. Opin. Plant Biol. 9, 322–330.
[2] Grotz, N. and Guerinot, M.L. (2006) Molecular aspects of Cu, Fe and Zn homeostasis in plants. Biochim. Biophys. Acta 1763, 595–608.
[3] Briat, J.F., Curie, C. and Gaymard, F. (2007) Iron utilization and metabolism in plants. Curr. Opin. Plant Biol. 10, 276–282.
[4] Römheld, V. and Marschner, H. (1986) Evidence for a specific uptake system for iron phytosiderophore in roots of grasses. Plant Physiol. 80, 175–180.
[5] Takagi, S. (1976) Naturally occurring iron-chelating compounds in oat- and rice-root washings. Soil Sci. Plant Nutr. 22, 423–433.
[6] Takemoto, T., Nomoto, K., Fushiya, S., Ouchi, R., Kusano, G., Hikino, H., Takagi, S., Matuura, Y. and Kakudo, M. (1978) Structure of mugineic acid, a new amino acid possessing an iron-chelating activity from roots washing of water-cultured *Hordeum vulgare* L.. Proc. Jpn. Acad. 54-B, 469–473.
[7] Ma, J.F. (2005) Plant root responses to three abundant soil mineral: silicon, aluminum and iron. Crit. Rev. Plant Sci. 24, 267–281.
[8] Inoue, H., Higuchi, K., Takahashi, M., Nakanishi, H., Mori, S. and Nishizawa, N.K. (2003) Three rice nicotianamine synthase genes, OsNAS1, OsNAS2, and OsNAS3 are expressed in cells involved in long-distance transport of iron and differentially regulated by iron. Plant J. 36, 366–381.
[9] Schaaf, G., Ludewig, U., Erenoglu, B.E., Mori, S., Kitahara, T. and von Wirén, N. (2004) ZmYS1 functions as a proton-coupled symporter for phytosiderophore- and nicotianamine-chelated metals. J. Biol. Chem. 279, 9091–9096.
[10] Takahashi, M., Terada, Y., Nakai, I., Nakanishi, H., Yoshimura, E., Mori, S. and Nishizawa, N.K. (2003) Role of nicotianamine in the intracellular delivery of metals and plant reproductive development. Plant Cell 15, 1263–1280.
[11] Curie, C., Panaviene, Z., Loulergue, C., Dellaporta, S.L., Briat, J.F. and Walker, E.L. (2001) Maize yellow stripe1 encodes a membrane protein directly involved in Fe(III) uptake. Nature 409, 346–349.
[12] Murata, Y., Ma, J.F., Yamaji, N., Ueno, D., Nomoto, K. and Iwashita, T. (2006) A specific transporter for iron(III)–phytosiderophore in barley roots. Plant J. 46, 563–572.
[13] Namba, K., Murata, Y., Horikawa, M., Iwashita, T. and Kusumoto, S. (2007) A practical synthesis of the phytosiderophore 2′-deoxymugineic acid: A key to the mechanistic study of iron acquisition by graminaceous plants. Angew. Chem. Int. Ed. 46, in press, doi:10.1002/anie.2007.02.403.
[14] Muñoz, V. and Serrano, L. (1995) Elucidating the folding problem of α-helical peptides using empirical parameters III: temperature and pH dependence. J. Mol. Biol. 245, 297–308.
[15] Sreerama, N. and Woody, R.W. (2000) Estimation of protein secondary structure from circular dichroism spectra: comparison of CONTIN, SELCON, and CDSSTR methods with an expanded reference set. Anal. Biochem. 287, 252–260.
[16] Hirokawa, T., Boon-Chieng, S. and Mitaku, S. (1998) SOSUI: classification and secondary structure prediction system for membrane proteins. Bioinformatics 14, 378–379.
[17] Koike, S., Inoue, H., Mizuno, D., Takahashi, M., Nakanishi, H., Mori, S. and Nishizawa, N.K. (2004) OsYSL2 is a rice metal-nicotianamine transporter that is regulated by iron and expressed in the phloem. Plant J. 39, 415–424.
[18] DiDonato Jr., R.J., Roberts, L.A., Sanderson, T., Eisley, R.B. and Walker, E.L. (2004) Arabidopsis *Yellow Stripe-Like2* (*YSL2*): a metal-regulated gene encoding a plasma membrane transporter of nicotianamine-metal complexes. Plant J. 39, 403–414.
[19] Schaaf, G., Schikora, A., Häberle, J., Vert, G., Ludewig, U., Briat, J.F., Curie, C. and von Wirén, N. (2005) A putative function for the *Arabidopsis* Fe–Phytosiderophore transporter homolog AtYSL2 in Fe and Zn homeostasis. Plant Cell Physiol. 46, 762–774.
[20] Le Jean, M., Schikora, A., Mari, S., Briat, J.F. and Curie, C. (2005) A loss-of-function mutation in *AtYSL1* reveals its role in iron and nicotianamine seed loading. Plant J. 44, 769–782.
[21] Waters, B.M., Chu, H.-H., Didonato, R.J., Roberts, L.A., Eisley, R.B., Lahner, B., Salt, D.E. and Walker, E.L. (2006) Mutations in Arabidopsis *yellow stripe-like1* and *yellow stripe-like3* reveal their roles in metal ion homeostasis and loading of metal ions in seeds. Plant Physiol. 141, 1446–1458.
[22] Hodoshima, H., Enomoto, Y., Shoji, K., Shimada, H., Goto, F. and Yoshihara, T. (2007) Differential regulation of cadmium-inducible expression of iron-deficiency-responsible genes in tobacco and barley. Physiol. Plantarum 129, 622–634.
[23] Gendre, D., Czernic, P., Conéjéro, G., Pianelli, K., Briat, J.F., Lebrun, M. and Mari, S. (2007) *TcYSL3*, a member of the *YSL* gene family from the hyper-accumulator *Thlaspi caerulescens*, encodes a nicotianamine-Ni/Fe transporter. Plant J. 49, 1–15.
[24] von Wirén, N., Klair, S., Bansal, S., Briat, J.F., Khodr, H., Shioiri, T., Leigh, R.A. and Hider, R.C. (1999) Nicotianamine

chelates both Fe^{III} and Fe^{II}. Implications for metal transport in plants. Plant Physiol. 119, 1107–1114.
[25] Ma, J.F., Kusano, G., Kimura, S. and Nomoto, K. (1993) Specific recognition of mugineic acid–ferric complex by barley roots. Phytochemistry 34, 599–603.
[26] Mori, S. (1999) Iron acquisition by plants. Curr. Opin. Plant Biol. 2, 250–253.
[27] Takahashi, M., Nakanishi, H., Kawasaki, S., Nishizawa, N.K. and Mori, S. (2001) Enhanced tolerance of rice to low iron availability in alkaline soils using barley nicotianamine aminotransferase genes. Nat. Biotechnol. 19, 466–469.
[28] Vasconcelos, M., Eckert, H., Arahana, V., Graef, G., Grusak, M.A. and Clemente, T. (2006) Molecular and phenotypic characterization of transgenic soybean expressing the *Arabidopsis* ferric chelate reductase gene, *FRO2*. Planta 224, 1116–1128.
[29] Ishimaru, Y., Kim, S., Tsukamoto, T., Oki, H., Kobayashi, T., Watanabe, S., Matsuhashi, S., Takahashi, M., Nakanishi, H., Mori, S. and Nishizawa, N.K. (2007) Mutational reconstructed ferric chelate reductase confers enhanced tolerance in rice to iron deficiency in calcareous soil. Proc. Natl. Acad. Sci. USA 104, 7373–7378.